

# Lipid Rafts Direct Macrophage Motility in the Tissue Microenvironment

MICHELLE L. PREVITERA,<sup>1,2</sup> KIMBERLY PETERMAN,<sup>1</sup> SMIT SHAH,<sup>1</sup> and JUAN LUZURIAGA<sup>1</sup>

<sup>1</sup>JFK Neuroscience Institute, JFK Medical Center, 65 James Street, Edison, NJ 08820, USA; and <sup>2</sup>Department of Neuroscience, Seton Hall University, 400 South Orange Avenue, South Orange, NJ 07079, USA

(Received 23 June 2014; accepted 23 September 2014; published online 1 October 2014)

Associate Editor Jennifer West oversaw the review of this article.

**Abstract**—Infiltrating leukocytes are exposed to a wide range of tissue elasticities. While we know the effects of substrate elasticity on acute inflammation *via* the study of neutrophil migration, we do not know its effects on leukocytes that direct chronic inflammatory events. Here, we studied morphology and motility of macrophages, the innate immune cells that orchestrate acute and chronic inflammation, on polyacrylamide hydrogels that mimicked a wide range of tissue elasticities. As expected, we found that macrophage spreading area increased as substrate elasticity increased. Unexpectedly, we found that morphology did not inversely correlate with motility. In fact, velocity of steady-state macrophages remained unaffected by substrate elasticity, while velocity of biologically stimulated macrophages was limited on stiff substrates. We also found that the lack of motility on stiff substrates was due to a lack of lipid rafts on the leading edge of the macrophages. This study implicates lipid rafts in the mechanosensory mechanism of innate immune cell infiltration.

**Keywords**—Elasticity, Stiffness, Migration, Innate immunity, Cell-mediated inflammation, Morphology, Cholesterol, Velocity, Acute inflammation, Chronic inflammation.

## INTRODUCTION

Leukocytes are present in every healthy and diseased tissue and are exposed to a varied range of tissue elasticities. For example, leukocytes present in adipose tissue experience 17 Pa of elasticity, whereas leukocytes present in tendons experience 310 MPa of elasticity.<sup>18</sup> Even within an organ system, elasticities of tissue are extremely diverse.<sup>5</sup> In the rat central nervous system, brain parenchyma is about 1 kPa while spinal cord parenchyma is about 27 kPa.<sup>18</sup> Furthermore, clinical studies have recently showed that these healthy

tissue elasticities are adversely affected by disease.<sup>36</sup> *In vitro* studies suggest that tissue elasticity alters as a result of disease states and directs neuron plasticity,<sup>25,26</sup> fibroblast migration,<sup>19</sup> and cardiomyocyte beating.<sup>6</sup>

Recent studies have also showed that tissue elasticity directs leukocytes migration<sup>12,13,22,29</sup> an initial inflammatory event for recruitment of leukocytes to the site of tissue damage.<sup>7,10</sup> For example, Oakes *et al.*<sup>22</sup> found that neutrophils migrated faster on soft gels, but more persistently and over longer distances on stiff substrates and Stroka *et al.*<sup>29</sup> found that neutrophil migration was biphasic with optimal elasticity migration dependent upon ligand concentration. However, these findings contradicted Jannat *et al.*'s findings, which showed neutrophil migration was unaffected by substrate elasticity unless a chemoattractant gradient is applied.<sup>12,13</sup> Regardless of the discrepancies among studies, which are most likely due to differences in the ranges of elasticities evaluated, these data all suggest that migration of leukocytes involved in acute inflammation (i.e. neutrophils) is elasticity dependent. However, investigations on elasticity-mediated migration of leukocytes involved in chronic inflammation (i.e. macrophages) are limited.

The cytoskeleton and associated proteins are known to regulate elasticity-mediated migration and overall morphology of cells.<sup>2,19,37</sup> Yet, the role of lipid rafts, which also promote migration and regulate the cytoskeleton,<sup>17,35</sup> in elasticity-mediated events is not yet been elucidated. Lipid rafts are microdomains found in plasma membranes that contain high concentrations of cholesterol and glycosphingolipids. They have been shown to promote migration of non-small cell lung cancer,<sup>14</sup> melanoma,<sup>33</sup> and intestinal epithelial cells<sup>32</sup> *via* cytoskeleton regulation. One report showed that the depletion of lipid rafts inhibited small cell lung cancer migration by inhibiting phosphorylation of key

Address correspondence to Michelle L. Previtera, JFK Neuroscience Institute, JFK Medical Center, 65 James Street, Edison, NJ 08820, USA. Electronic mail: mprevitera@jfkhealth.org

regulatory cytoskeletal proteins.<sup>14</sup> Another report showed that lipid rafts mediated integrin  $\beta 1$  internalization in migrating intestinal epithelial cells.<sup>32</sup> Interestingly, another report showed that lipid raft content modulated cell elasticity,<sup>3</sup> suggesting that lipid rafts play a role in mechanotransduction. Collectively, these studies support the relationship between lipid rafts, cytoskeleton, and cell elasticity and strongly suggest an integral role for lipid rafts in the regulation of elasticity-mediated migration.

In this study, we elucidated the role of lipid rafts in macrophage motility on elastic substrates to reveal the influences of biophysical cues on leukocytes involved in chronic inflammation and define new mechanosensing mechanisms. We hypothesized that lipid raft depletion limits macrophage motility on stiff substrates, which represent diseased tissues. To test this hypothesis, peripheral macrophages were grown on polyacrylamide gels that mimicked the elasticities of diseased and healthy tissues. Since macrophages are initially in a steady-state and become activated by harmful biological stimulants, macrophages were grown in both a steady state and a stimulated state to best understand how the two macrophage states respond to biophysical cues. Time-lapse images were taken and velocities and trajectories were measured. To determine the involvement of lipid rafts in elasticity-mediated motility, lipid raft formation was inhibited and macrophage motility was measured. This study suggests that elasticity-mediated lipid raft depletion governs migratory events.

## MATERIALS AND METHODS

### *Polyacrylamide Hydrogel Preparation and Functionalization*

0.3, 1, 6, 27, 47, 120, and 230 kPa polyacrylamide hydrogels (gels) were prepared, as previously described.<sup>24</sup> Briefly, 12-mm round glass coverslips were treated with (3-aminopropyl)-trimethoxysilane. After 3 min the coverslips were rinsed extensively. Next, coverslips were treated with 0.05% glutaraldehyde for 30 min. 3, 4, 5, 8, 10, 15, and 20% acrylamide:bis-acrylamide solutions were prepared with deionized water and tetramethylethylenediamine (TEMED) and ammonium persulfate (APS) was then added to solutions to polymerize the gels. After adding APS and TEMED but prior to polymerization, 25  $\mu$ l of solution was dispensed onto the treated coverslip. In order for the topology to form evenly, a coverslip treated with RainX<sup>TM</sup> (Houston, TX) was placed on top of each gel and removed once the gel was polymerized. Gels were allowed to polymerize for 10 min. Gels were

thoroughly rinsed with 0.2 M HEPES buffer, pH 8.5 for a minimum of 24 h to remove unpolymerized acrylamide monomers. Finally, gels were sterilized for 30 min under UV light.

Inert gels were functionalized to allow for cell adhesion. Twice, sulfo-SANPAH (0.315 mg/ml in water; ProteoChem, Loves Park, IL) was placed on each gel and the gels were exposed to UV light for 5 min. Gels were rinsed and incubated with poly-D-lysine (0.2 mg/ml in water) for 60 min at room temperature. Gels were then rinsed and equilibrated with media for 30 min at 37 °C. Media was composed of DMEM/F12 (Invitrogen, Carlsbad, CA) containing 10% fetal bovine serum and 1% penicillin/streptomycin (P/S).

### *Bone Marrow-Derived Macrophage (BMM) Cultures*

All animal protocols were approved by the Institutional Animal Care and Use Committee, a shared committee between Seton Hall University and the JFK Neuroscience Institute at JFK Medical Center. Monocytes were harvested and differentiated into macrophages, as previously described.<sup>38</sup> Briefly, bone marrow cells were extracted from femurs and tibias harvested from 12<sup>+</sup>-week old C57BL/6 mice. Cells were plated onto petri dishes in BMM media supplemented with 20–40 ng/ml of macrophage-colonizing stimulating factor (eBioscience, San Diego, CA). Media was changed every 3 days. After 6–7 days, cells were trypsinized, then plated onto gels and treated with and without 10 ng/ml of lipopolysaccharide (LPS). Cultures were maintained at 37 °C with 5% CO<sub>2</sub>.

### *Morphology and Lipid Raft Analysis*

25,000 cells/cm<sup>2</sup> were plated onto all gels. After 18–24 h, live images were captured using a TE200 microscope (Nikon, Tokyo, Japan) with a 10 $\times$  objective, a QI-Click digital CCD camera, and Q-Capture software (Q-Imaging, Surrey, BC, Canada). Images were analyzed using ImageJ software (NIH, Bethesda, MD).<sup>24</sup> Three random images per gel were captured and images possessing gel defects were discarded in the analysis process. Morphologically circular and noncircular cells were defined in Fig. 1. The experimenter was blinded during the measurement process to prevent bias.

For lipid raft analysis, cells were fixed with 4% paraformaldehyde for 15 min at room temperature. Cells were then blocked with 5% normal goat serum in PBS and stained with cholera toxin subunit B conjugated with Alexa 488 (Invitrogen). Gels were imaged at the same exposure time with a 10 $\times$  objective. Fluorescence intensities were measured using ImageJ software. Background was subtracted from the intensities

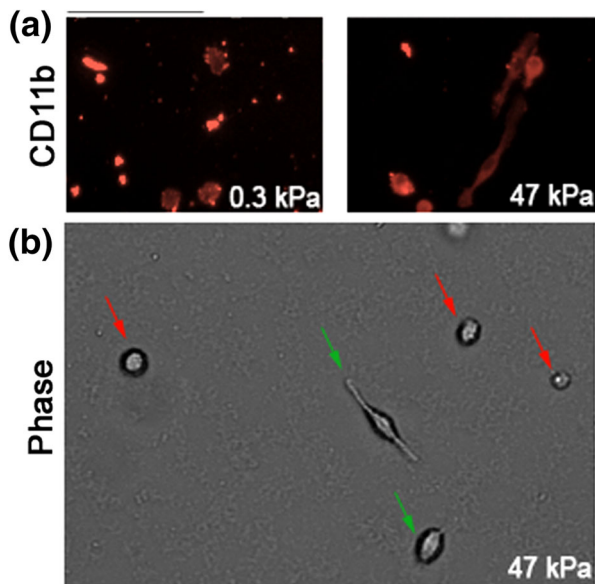


**FIGURE 1.** Bone marrow-derived macrophages (BMMs) on gels. (a) Cells on gels immunostained with macrophage marker CD11b. Immunostaining shows that the cells with different morphologies on 0.3 and 47 kPa gels were macrophages. (b) Phase contrast images of BMMs. Images show two distinguishable BMM morphologies. Green arrows indicate non-circular BMMs and red arrows indicate non-polarized BMMs on a 47 kPa gel. These populations were quantified for all gels in Fig. 2.

and each biological replicate was normalized by the average intensity of 0.3 kPa control conditions to account for staining differences between experiments. The experimenter was blinded during the measurement process to prevent bias.

#### *Motility Analysis*

25,000–50,000 cells/cm<sup>2</sup> were plated onto 0.3 and 230 kPa gels. For some LPS-treated cells, 1 mM of methyl-beta-cyclodextrin (M $\beta$ CD) was added to the media at the time of plating. 15–30 min after plating, images were captured in 30 s intervals for 30–60 min with a 40 $\times$  objective. ImageJ software compiled sequences. Cell trajectories were traced and analyzed using the ImageJ plugins ‘Manual Tracking’ and ‘Chemotaxis and Migration Tool’ (Ibidi, Verona, WI), respectively. A fixed point on the gel, typically a gel defect, was also tracked and any gel movement was eliminated from the experimental values. Cell velocity was measured as the average distance the cells traveled over time. The experimenter was blinded during the measurement process to prevent bias.

#### *Statistical Analysis*

Data was pooled from a minimum of three animals. Excluding trajectory maps, data is presented on graphs

as mean  $\pm$  SEM. \* $p$  < 0.05, \*\* $p$  < 0.01 and \*\*\* $p$  < 0.001 as determined by Kruskal–Wallis followed by Dunn’s Multiple Comparison Test. N<sub>subtext</sub> indicates the number of images, cells, or wells and the subtext refers to the condition. Scale bars are 0.1 mm.

## RESULTS

Since the effect of substrate elasticity on macrophage migration has not yet been studied, we first evaluated morphology, velocity, and directionality of both biologically stimulated (LPS-treated) and steady-state (control) macrophages.

### *Macrophages Adopt a Longer and Larger Morphology on Stiff Substrates*

Oakes *et al.* found that upon initial plating of neutrophils on 5–50 kPa polyacrylamide hydrogels, the spreading area of neutrophils increased as substrate stiffness increased. This morphology inversely correlated with cell speed, which was slower on stiffer substrates.<sup>22</sup> Since this study showed morphology is a key indicator of leukocyte motility, we first evaluated BMM morphology and spreading area. BMMs plated on gels were either biologically stimulated with LPS or remained in a steady state by treating with vehicle control. Unlike neutrophils, macrophages are exclusively found in tissues and are already exposed to tissue elasticity prior to activation. Therefore, BMMs were imaged on gels after exposure to substrate elasticity for a period of time (18–24 h).

Two distinctive morphologies were present on the gels (Fig. 1): a circular morphology and noncircular morphology. Both morphologies were positive for the macrophage marker CD11b (Fig. 1a) and both morphologies were found on all gels (Figs. 1b and 2). A higher percentage of circular BMMs were present on 0.3–27 kPa gels, while a higher percentage of noncircular BMMs were present on 47–230 kPa gels (Fig. 2a). Circular BMM areas increased as substrate elasticity increased (Fig. 2b) and noncircular BMM areas and aspect ratios (AR) increased as substrate elasticity increased (Figs. 2c and 2d, respectively). Phenotypes occurred regardless of LPS treatment indicating stiffer gels promoted cell spreading and elongation independent of LPS stimulation.

### *Motility is Dependent on Both Substrate Elasticity and Macrophage State*

Numerous reports have shown that an increase in spreading area is inversely correlated to cell motility.<sup>19,22</sup> However, in the presence of a biological

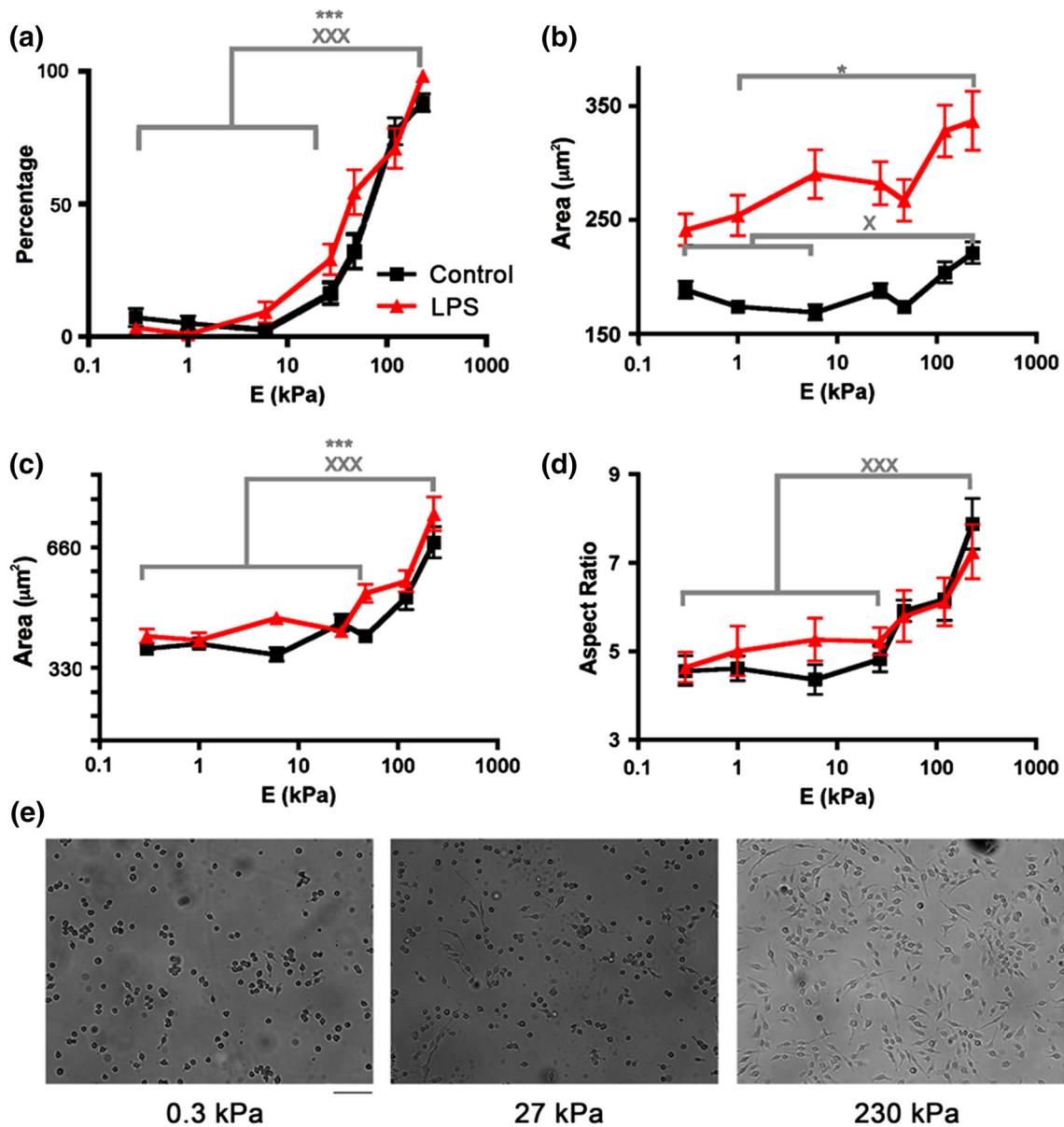


**FIGURE 2.** BMM morphology on 0.3–230 kPa gels. (a) Noncircular percentages of vehicle control- (control) and LPS-treated BMMs. The percentage of noncircular control- (black) and LPS-treated (red) BMMs increased as gel elasticity increased. (b) Circular areas of control- and LPS-treated BMMs. The areas of control- and LPS-treated BMMs increased as gel elasticity increased. (c) Noncircular areas of control- and LPS-treated BMMs. The areas of control- and LPS-treated BMMs increased as gel elasticity increased. (d) Noncircular aspect ratio (AR) of control- and LPS-treated BMMs. AR of control- and LPS-treated BMMs increased as gel elasticity increased. (e) Image representation of graphs (a–d). A minimum of 21 images or 20 cells were analyzed for each gel condition. (\*) and (x) indicates statistical significance for LPS-treated BMMs and control BMMs, respectively.

stimulant such as LPS, macrophages are known to have increased motility.<sup>15</sup> Therefore, we asked what are the independent and combined effects of elasticity and LPS? We chose to examine BMM motility on 0.3 and 230 kPa gels since circular and noncircular cell populations were the most homogenous on these two gels. This ensured that morphologically heterogeneous populations did not cause heterogeneous motility and allowed for morphology and motility correlations.

Our velocity data did not strictly adhere to the morphology–motility paradigm, where morphology inversely correlates to motility. The velocity of control BMMs on 0.3 kPa gels was not significantly different from the velocity of control BMMs on 230 kPa gels (Fig. 3a). However, LPS-treated BMMs on 230 kPa gels exhibited a significant decrease in velocity compared to LPS-treated BMMs on 0.3 kPa. In addition, the velocity of LPS-treated BMMs on 230 kPa was

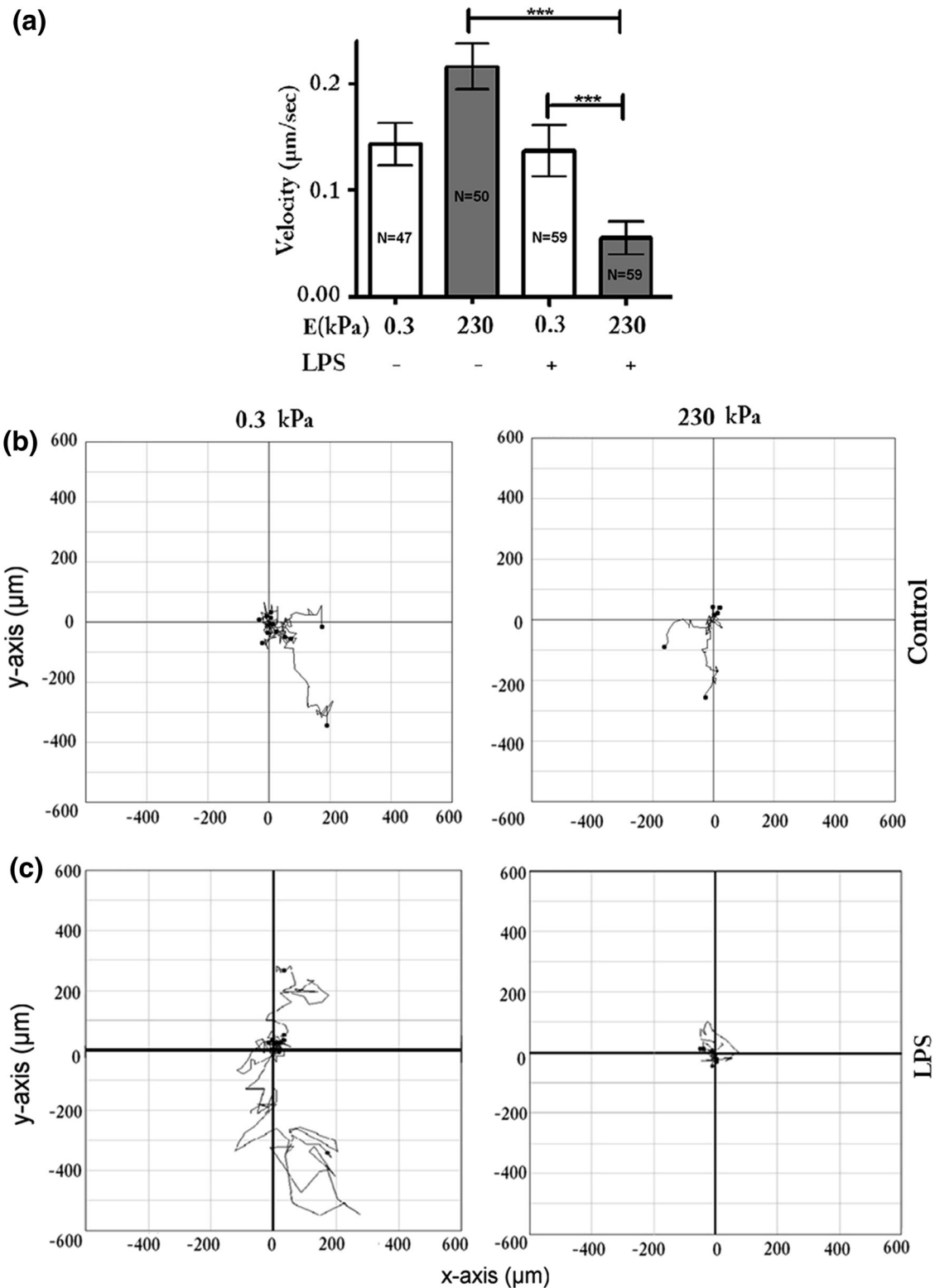


**FIGURE 3.** BMM velocity on 0.3 and 230 kPa gels. (a) BMM velocity. BMMs were plated on 0.3 (white bars) and 230 kPa (grey bars) gels and treated with vehicle control (control) or LPS. The graph shows no significant difference between control BMM on 0.3 and 230 kPa gels. However, the presence of LPS decreased BMM velocity on 230 kPa gels. (b) and (c) Representative trajectory maps of (a). Maps show displacement of control (b) and LPS-treated BMMs (c) on 0.3 (left) and 230 (right) kPa gels.

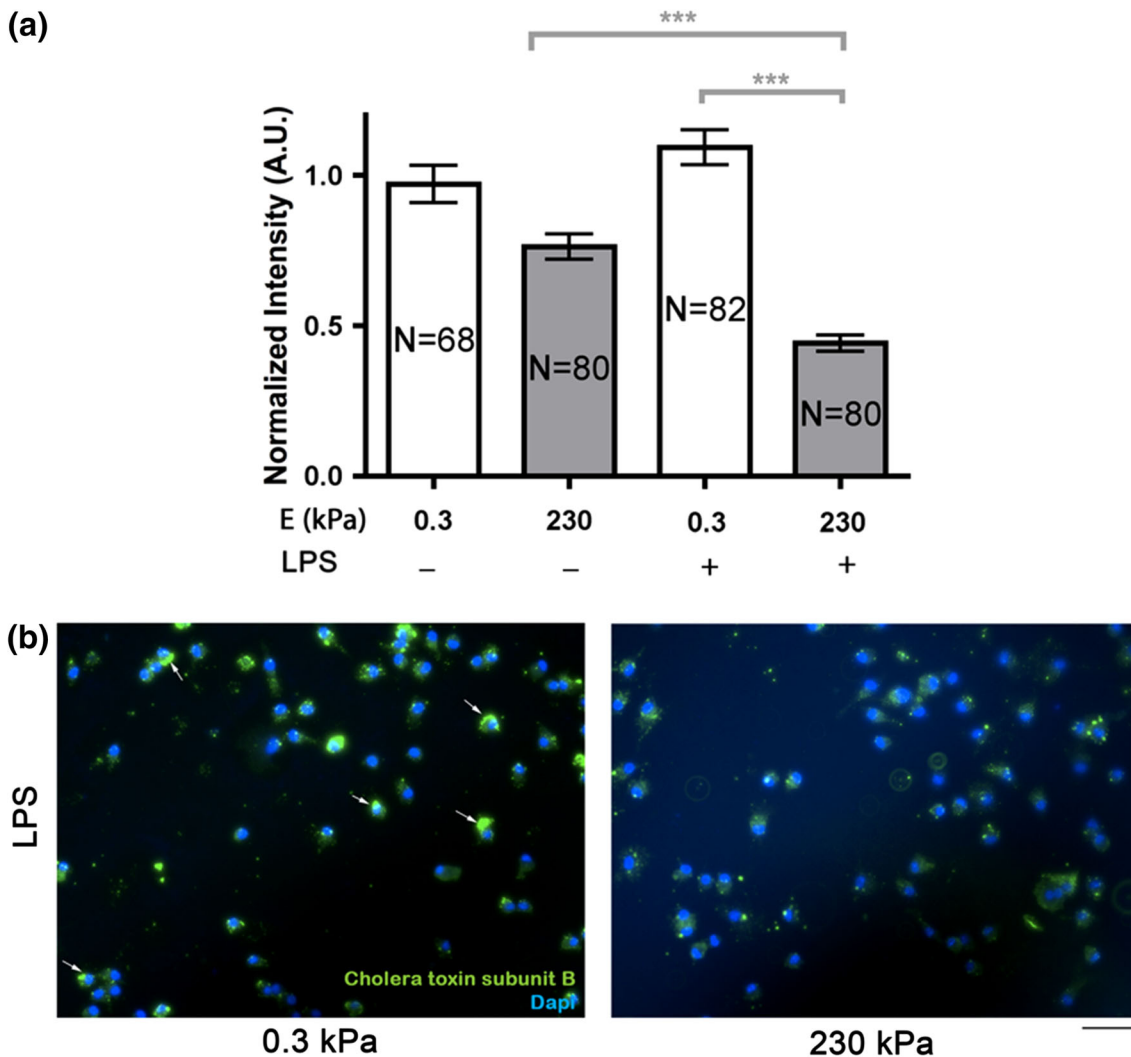


**FIGURE 4.** Lipid raft distribution. (a) BMMs stained for lipid rafts. Graph shows cholera toxin subunit B staining intensity decreased for LPS-treated BMM grown on 230 kPa gels. (b) Representative images of (a). Images show cholera toxin B staining (green) and DAPI staining (blue) on 0.3 (left) and 230 kPa (right) gels. White arrows on 0.3 kPa images indicate increases in cholera toxin B staining and show the asymmetrical patterning of staining.

significantly decreased compared to control BMMs on 230 kPa gels. Trajectories were also measured to determine directional movement, but trajectory maps showed random motion (Fig. 3b). These data indicate that BMM motility follows the morphology–motility paradigm only when a biological stimulant is present.

#### *Lipid Rafts are Involved in Elasticity-Mediated Motility*

Next, we sought to define the role of lipid rafts in elasticity-mediated macrophage migration. We hypothesized that LPS-treated macrophages on 230 kPa gels lacked lipid rafts since lipid rafts promote migration. To test this hypothesis, we first examined lipid raft content for all conditions. We stained lipid rafts using cholera toxin subunit B, which attaches to cells by binding to gangliosides. We found a lower intensity of

lipid raft staining for LPS-treated BMMs grown on 230 kPa gels compared to all other conditions (Fig. 4a). We also examined the distribution of the staining. Migrating cells are typically asymmetrical, with one end having a leading edge that exhibits protrusion and the opposite end having a rear edge that undergoes retraction. We observed that lipid raft distribution in LPS-treated BMMs on 0.3 kPa gels was asymmetrical; specifically, a higher intensity was observed on the leading edge (Fig. 4b). These data suggest that lipid rafts in LPS-treated BMMs on 0.3 kPa substrates promote BMM motility.

To further confirm the role of lipid rafts in macrophage motility on soft substrates, we depleted lipid rafts by incubating LPS-treated BMMs with M $\beta$ CD, a chemical that disrupts lipid raft integrity by depleting cholesterol (Fig. 5). We found that in the

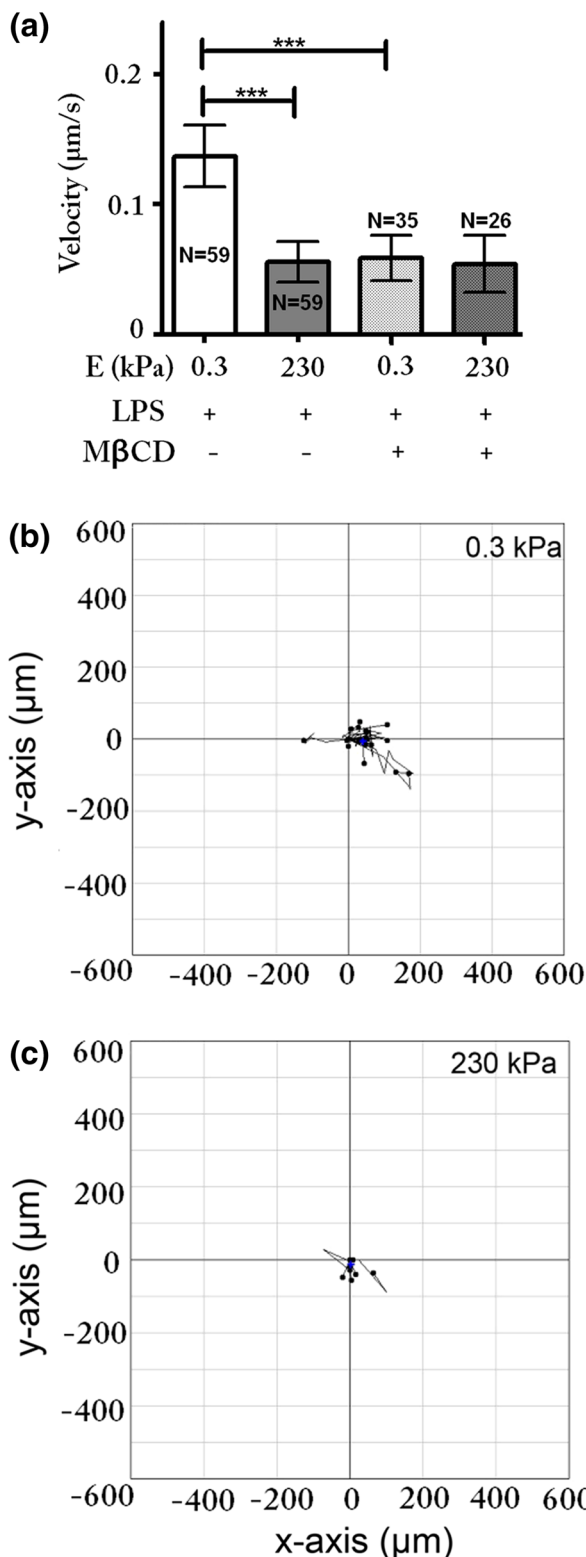


**FIGURE 5.** Effect of M $\beta$ CD on BMM velocity: (a) Velocity of BMMs treated with M $\beta$ CD and LPS. BMM velocity decreased on 0.3 and 230 kPa gels in the presence of M $\beta$ CD. (b) and (c) Representative trajectory maps of M $\beta$ CD-treated BMMs on 0.3 (b) and 230 (c) kPa gels.

presence of M $\beta$ CD, LPS-treated BMMs on 0.3 kPa gels had no difference in velocity compared to LPS-treated BMMs on 230 kPa gels. However, LPS-treated BMMs incubated in M $\beta$ CD on 0.3 kPa gels had a significant decrease in velocity compared to LPS-treated BMMs incubated with no M $\beta$ CD on 0.3 kPa gels. Collectively, staining and migration data indicate lipid rafts are vital to migration and lack of lipid rafts may be responsible for the lack of migration on 230 kPa gels.

## DISCUSSION

Unlike neutrophils, where a rapid response to tissue elasticity is crucial for recruitment since neutrophils are primarily recruited from circulation, rapid response to tissue elasticity is less essential for macrophage recruitment since a residential population of macrophages is present prior to tissue damage. Because of this, macrophages are exposed to tissue elasticity prior to initiation of inflammatory events.<sup>23</sup> Therefore, in this study, cells were allowed to adhere onto elastic substrates and acclimate to the substrate for a minimum of 10 min prior to examining macrophage motility or morphology. This is in contrast to previous innate immune cell studies, where morphology and motility behaviors were measured immediately after adhesion.<sup>22</sup>

### Morphology

Our morphology studies showed that macrophages on soft substrates had a higher population of small, round macrophages whereas stiff substrates had a higher population of large, long macrophages (Figs. 1 and 2). This was consistent with other reports that have shown fibroblasts,<sup>19,37</sup> neutrophils,<sup>22</sup> and astrocytes<sup>8</sup> spread more on stiffer substrates. However, our results followed an unusual exponential curve, where most macrophages are small and round on substrates below 47 kPa. This finding suggests that a specific elasticity threshold is required for macrophage elongation and spreading. This threshold was present regardless of the activation state. Therefore, steady-state and stimulated macrophages were anticipated to have similar motility behaviors. Furthermore, an inverse correlation between motility and morphology was anticipated since cells with a large spreading area require more time for adhesion disruption due to the increase in contact.<sup>22</sup> As discussed below, the morphology–motility paradigm was only applicable to macrophages stimulated with LPS in our studies.

### Motility

In motility studies, we found that stimulated and steady-state macrophages responded differently to soft and stiff substrates. Specifically, macrophages were relatively mobile unless grown on stiff substrates in the presence of a biological stimulant (i.e. LPS). In addition, cells had no directional movement in any condition, most likely due to the uniformity of gel elasticity and stimulant. The inclusion of physiological features such as the presence of a chemoattractant<sup>13</sup> or stiffness<sup>11</sup> gradient, both known to increase directional movement of cells in a stiffness dependent manner, would modulate directional movement. Most importantly, our motility study revealed that the morphology–motility paradigm was limited because of macrophages role in both acute and chronic inflammation.

The ability of macrophages to maintain a long-term presence in both healthy and damaged tissues allows them to orchestrate acute and chronic inflammation. However, this establishes a dichotomy in motility behavior; macrophages need to migrate to the site of tissue damage in the acute phase of inflammation and then macrophages need to remain immobile for a period of time to orchestrate chronic inflammatory events at the site of tissue damage. Here, we reported that this migration dichotomy was regulated by the elasticity of the environment. Macrophages remained relatively mobile on all substrates when a biological stimulant was absent and macrophages remained mobile on substrates mimicking healthy tissue elasticity when a biological stimulant was present (Fig. 3). This suggests that steady-state macrophages remain mobile to scan the site for biological stimulants regardless of the physical environment and stimulated macrophages remain mobile to be recruited to the site of tissue damage. The presence of a biological stimulant limited macrophage motility in conditions that mimic the elasticity of diseased tissues, which is  $\geq 47$  kPa.<sup>1,4,21,27,30</sup> This limitation in motility by the physical properties of the diseased-tissue allows for orchestration of inflammation at the site of tissue damage.

While substrate elasticity regulates this dichotomy, the morphology–motility paradigm becomes limited. Our data showed that steady-state macrophages did not adhere to the morphology–motility paradigm, while stimulated macrophages did adhere to the morphology–motility paradigm. This indicates that morphology is not always an indicator of function and function, specifically migration, should not be assumed based on cell morphology.

Our study challenges the morphology–motility paradigm and disagrees with other studies most likely

because previous studies examined migration on a more limited range of gel elasticity. Our motility study included substrates that mimicked extremely soft tissues such as adipose and brain tissues (0.3–1 kPa) and substrates that mimicked extremely stiff tissues such as muscle and diseased tissues (27–230 kPa).<sup>18</sup> For example, Oakes *et al.*'s study, which showed that neutrophils were slower and more persistent on stiff substrates, included substrates in the intermediate elasticity range (5–100 kPa).<sup>22</sup> Stroka *et al.*'s study, which showed neutrophil speed was biphasic on substrates, also included substrates in the intermediate elasticity range (3–13 kPa).<sup>29</sup> Jannat *et al.*'s study included softer substrates but not stiffer substrates (1–40 kPa) and reported that neutrophils had no difference in velocity or directionality among substrates.<sup>13</sup> The exclusion of substrates  $< 3$  and  $> 40$  kPa in these studies may account for discrepancies with our data. This suggests that motility studies should include substrates that mimic the elasticity of both extremely soft and stiff tissues since the motility–morphology paradigm is sensitive to the range of elasticity investigated. However, work from the Gonzalez lab included extremely softer substrates (1–6 kPa) and agreed with our results. They reported that soft matrices promoted chemotaxis.<sup>16</sup> However, these matrices were biologically and mechanically more indicative of the microenvironment since the elastic PEG hydrogel models were conjugated with ECM proteins and were 3D. Studies that include substrates and matrices that are more physiologically indicative of the microenvironment, i.e. include both biological and mechanical features, will be vital to further elucidating the role of mechanotransduction mechanisms in leukocyte motility.

### Lipid Rafts

To fully understand macrophage motility, the molecular mechanisms involved must be explored. We chose to investigate lipid rafts because they are known to mediate LPS recognition,<sup>31</sup> promote cell motility<sup>14,32,33</sup> and modulate cell stiffness on elastic substrates.<sup>3</sup> Lipid raft staining showed lower amounts of lipid rafts in stimulated macrophages grown on 230 kPa gels compared to all other conditions (Fig. 4a). Interestingly, lipid raft staining directly correlated to motility results. In addition, M $\beta$ CD treatment eliminated motility on 0.3 kPa gels (Fig. 5), confirming that lipid rafts promote migration on soft substrates. Since cells are known to adapt to substrate elasticity, we speculated that macrophages are softening in an attempt to match the elasticity of the soft substrates<sup>28</sup> and, as a result, lipid raft formation enhanced from softening promoted cell motility.



Lipid rafts on the leading edge of cells promote migration by redistributing critical proteins.<sup>9,20</sup> Here, we showed that lipid rafts were on the leading edge of stimulated macrophages grown on 0.3 kPa gels (Fig. 4b, arrows). This asymmetrical membrane distribution may result in enrichment of mechanosensors and machinery that propels the cells forward at the leading edge. In fact, one study showed that lipid rafts facilitate integrin  $\beta 1$  clustering, a key step in cell migration.<sup>34</sup> Further investigations on the receptors that asymmetrically cluster and facilitate migration are needed to fully understand the role of lipid raft formation in elasticity-mediated migration.

### CONCLUSION

In conclusion, an elastic threshold directs macrophage morphology, but morphology does not always indicate motility behavior. Macrophages grown on gels below 47 kPa are typically smaller and rounder than macrophages grown on gels above 47 kPa. The two morphological populations do not always follow the typical morphology–motility paradigm, where leukocytes with larger spreading areas are less mobile than leukocytes with smaller spreading areas. We found no differences in motility for steady-state macrophages, but macrophages adhere to this paradigm upon LPS stimulation; i.e. LPS-treated macrophages had limited motility on 230 kPa gels compared to macrophages on 0.3 kPa gels. We also found that asymmetrical formation of lipid rafts contributes to motility of LPS-treated macrophages on 0.3 kPa gels. This suggests that inhibition of motility of LPS-treated macrophages on 230 kPa gels may be the result of lipid raft depletion and lack of asymmetrical lipid raft formation. In conclusion, lipid rafts attenuate motility of stimulated macrophages to allow macrophages to orchestrate inflammation at the site of tissue damage.

### ACKNOWLEDGMENTS

Thank you to Mason Hui and Norell Hadzimichalis for editing this manuscript. Funding was provided by the JFK Neuroscience Institute and the JFK Foundation.

### CONFLICT OF INTEREST

Authors declare no conflict of interest.

### REFERENCES

- Baldewising, R. A., J. A. Schaar, F. Mastik, and A. F. van der Steen. Local elasticity imaging of vulnerable atherosclerotic coronary plaques. *Adv. Cardiol.* 44:35–61, 2007.
- Beningo, K. A., M. Dembo, I. Kaverina, J. V. Small, and Y. L. Wang. Nascent focal adhesions are responsible for the generation of strong propulsive forces in migrating fibroblasts. *J. Cell Biol.* 153:881–888, 2001.
- Byfield, F. J., H. Aranda-Espinoza, V. G. Romanenko, G. H. Rothblat, and I. Levitan. Cholesterol depletion increases membrane stiffness of aortic endothelial cells. *Biophys. J.* 87:3336–3343, 2004.
- de Korte, C. L., A. F. van der Steen, E. I. Cepedes, G. Pasterkamp, S. G. Carlier, F. Mastik, A. H. Schoneveld, P. W. Serruys, and N. Bom. Characterization of plaque components and vulnerability with intravascular ultrasound elastography. *Phys. Med. Biol.* 45:1465–1475, 2000.
- Elkin, B. S., A. I. Ilankovan, and B. Morrison, 3rd. A detailed viscoelastic characterization of the p17 and adult rat brain. *J. Neurotrauma* 28:2235–2244, 2011.
- Engler, A. J., C. Carag-Krieger, C. P. Johnson, M. Raab, H. Y. Tang, D. W. Speicher, J. W. Sanger, J. M. Sanger, and D. E. Discher. Embryonic cardiomyocytes beat best on a matrix with heart-like elasticity: Scar-like rigidity inhibits beating. *J. Cell Sci.* 121:3794–3802, 2008.
- Fraser, I. P., H. Koziel, and R. A. Ezekowitz. The serum mannose-binding protein and the macrophage mannose receptor are pattern recognition molecules that link innate and adaptive immunity. *Semin. Immunol.* 10:363–372, 1998.
- Georges, P. C., W. J. Miller, D. F. Meaney, E. S. Sawyer, and P. A. Janmey. Matrices with compliance comparable to that of brain tissue select neuronal over glial growth in mixed cortical cultures. *Biophys. J.* 90:3012–3018, 2006.
- Gomez-Mouton, C., J. L. Abad, E. Mira, R. A. Lacalle, E. Gallardo, S. Jimenez-Baranda, I. Illa, A. Bernad, S. Manes, and A. C. Martinez. Segregation of leading-edge and uropod components into specific lipid rafts during t cell polarization. *Proc. Natl. Acad. Sci. USA* 98:9642–9647, 2001.
- Gordon, S. Pattern recognition receptors: doubling up for the innate immune response. *Cell* 111:927–930, 2002.
- Isenberg, B. C., P. A. Dimilla, M. Walker, S. Kim, and J. Y. Wong. Vascular smooth muscle cell durotaxis depends on substrate stiffness gradient strength. *Biophys. J.* 97:1313–1322, 2009.
- Jannat, R. A., M. Dembo, and D. A. Hammer. Traction forces of neutrophils migrating on compliant substrates. *Biophys. J.* 101:575–584, 2011.
- Jannat, R. A., G. P. Robbins, B. G. Ricart, M. Dembo, and D. A. Hammer. Neutrophil adhesion and chemotaxis depend on substrate mechanics. *J. Phys.* 22:194117, 2010.
- Jeon, J. H., S. K. Kim, H. J. Kim, J. Chang, C. M. Ahn, and Y. S. Chang. Lipid raft modulation inhibits nsccl cell migration through delocalization of the focal adhesion complex. *Lung Cancer* 69:165–171, 2012.
- Kleveta, G., K. Borzecka, M. Zdioruk, M. Czerkies, H. Kuberczyk, N. Sybirna, A. Sobota, and K. Kwiatkowska. Lps induces phosphorylation of actin-regulatory proteins leading to actin reassembly and macrophage motility. *J. Cell. Biochem.* 113:80–92, 2012.
- Lauridsen, H. M., B. J. Walker, and A. L. Gonzalez. Chemically- and mechanically-tunable porous polyethyl-

- ene glycol gels for leukocyte integrin independent and dependent chemotaxis. *Technology* 2:133–143, 2014.
- <sup>17</sup>Leitinger, B., and N. Hogg. The involvement of lipid rafts in the regulation of integrin function. *J. Cell Sci.* 115:963–972, 2002.
- <sup>18</sup>Levental, I., P. Georges, and P. Janmey. Soft biological materials and their impact on cell function. *Soft Tissue Matter* 3:299–306, 2007.
- <sup>19</sup>Lo, C. M., H. B. Wang, M. Dembo, and Y. L. Wang. Cell movement is guided by the rigidity of the substrate. *Biophys. J.* 79:144–152, 2000.
- <sup>20</sup>Manes, S., E. Mira, C. Gomez-Mouton, R. A. Lacalle, P. Keller, J. P. Labrador, and A. C. Martinez. Membrane raft microdomains mediate front-rear polarity in migrating cells. *EMBO J.* 18:6211–6220, 1999.
- <sup>21</sup>Matsumoto, T., H. Abe, T. Ohashi, Y. Kato, and M. Sato. Local elastic modulus of atherosclerotic lesions of rabbit thoracic aortas measured by pipette aspiration method. *Physiol. Meas.* 23:635–648, 2002.
- <sup>22</sup>Oakes, P. W., D. C. Patel, N. A. Morin, D. P. Zitterbart, B. Fabry, J. S. Reichner, and J. X. Tang. Neutrophil morphology and migration are affected by substrate elasticity. *Blood* 114:1387–1395, 2009.
- <sup>23</sup>Previtera, M. Mechanotransduction in the immune system. *Cell. Mol. Bioeng.* 2014. doi:10.1007/s12195-014-0338-7.
- <sup>24</sup>Previtera, M. L., M. Hui, D. Verma, A. J. Shahin, R. Schloss, and N. A. Langrana. The effects of substrate elastic modulus on neural precursor cell behavior. *Ann. Biomed. Eng.* 41:1193–1207, 2013.
- <sup>25</sup>Previtera, M. L., C. G. Langhammer, and B. L. Firestein. Effects of substrate stiffness and cell density on primary hippocampal cultures. *J. Biosci. Bioeng.* 110:459–470, 2010.
- <sup>26</sup>Previtera, M. L., C. G. Langhammer, N. A. Langrana, and B. L. Firestein. Regulation of dendrite arborization by substrate stiffness is mediated by glutamate receptors. *Ann. Biomed. Eng.* 38:3733–3743, 2010.
- <sup>27</sup>Schaar, J. A., C. L. De Korte, F. Mastik, C. Strijder, G. Pasterkamp, E. Boersma, P. W. Serruys, and A. F. Van Der Steen. Characterizing vulnerable plaque features with intravascular elastography. *Circulation* 108:2636–2641, 2003.
- <sup>28</sup>Solon, J., I. Levental, K. Sengupta, P. C. Georges, and P. A. Janmey. Fibroblast adaptation and stiffness matching to soft elastic substrates. *Biophys. J.* 93:4453–4461, 2007.
- <sup>29</sup>Stroka, K. M., and H. Aranda-Espinoza. Neutrophils display biphasic relationship between migration and substrate stiffness. *Cell Motil. Cytoskelet.* 66:328–341, 2009.
- <sup>30</sup>Tracqui, P., A. Broisat, J. Toczek, N. Mesnier, J. Ohayon, and L. Riou. Mapping elasticity moduli of atherosclerotic plaque *in situ* via atomic force microscopy. *J. Struct. Biol.* 174:115–123, 2011.
- <sup>31</sup>Triantafilou, M., K. Miyake, D. T. Golenbock, and K. Triantafilou. Mediators of innate immune recognition of bacteria concentrate in lipid rafts and facilitate lipopolysaccharide-induced cell activation. *J. Cell Sci.* 115:2603–2611, 2002.
- <sup>32</sup>Vassilieva, E. V., K. Gerner-Smidt, A. I. Ivanov, and A. Nusrat. Lipid rafts mediate internalization of beta1-integrin in migrating intestinal epithelial cells. *Am. J. Physiol.* 295:G965–G976, 2008.
- <sup>33</sup>Wang, R., J. Bi, K. K. Ampah, X. Ba, W. Liu, and X. Zeng. Lipid rafts control human melanoma cell migration by regulating focal adhesion disassembly. *Biochim. Biophys. Acta* 3195–3205:2013, 1833.
- <sup>34</sup>Wang, R., J. Bi, K. K. Ampah, C. Zhang, Z. Li, Y. Jiao, X. Wang, X. Ba, and X. Zeng. Lipid raft regulates the initial spreading of melanoma a375 cells by modulating beta1 integrin clustering. *Int. J. Biochem. Cell Biol.* 45:1679–1689, 2013.
- <sup>35</sup>Wickstrom, S. A., K. Alitalo, and J. Keski-Oja. Endostatin associates with lipid rafts and induces reorganization of the actin cytoskeleton *via* down-regulation of RhoA activity. *J. Biol. Chem.* 278:37895–37901, 2003.
- <sup>36</sup>Wuerfel, J., F. Paul, B. Beierbach, U. Hamhaber, D. Klatt, S. Papazoglou, F. Zipp, P. Martus, J. Braun, and I. Sack. Mr-elastography reveals degradation of tissue integrity in multiple sclerosis. *Neuroimage* 49:2520–2525, 2010.
- <sup>37</sup>Yeung, T., P. C. Georges, L. A. Flanagan, B. Marg, M. Ortiz, M. Funaki, N. Zahir, W. Ming, V. Weaver, and P. A. Janmey. Effects of substrate stiffness on cell morphology, cytoskeletal structure, and adhesion. *Cell Motil. Cytoskelet.* 60:24–34, 2005.
- <sup>38</sup>Zhang, X., R. Goncalves, and D. M. Mosser. The isolation and characterization of murine macrophages (Chap. 14: Unit 14). *Curr. Protoc. Immunol.* 11:14, 2008.